Electronic Supplementary Information

Energy storage devices based on an endoskeleton structuring

Inho Nam,[ab] Jongseok Park,[a] Seongjun Bae,[a] Soomin Park,[ac] Young Geun Yoo,[a] Jongheop Yi*[a]

[a]School of Chemical and Biological Engineering, WCU Program of C_2E_2, ICP, Seoul National University, Seoul 08826, Republic of Korea.

[b]Present addresses: Centre for Plant Aging Research, Institute of Basic Science (IBS), Daegu 42988, Republic of Korea and Department of Chemistry, Stanford University, Stanford, California 94305, United States.

[c]Present address: Department of Chemistry, University of California, Berkeley, California 94705, Unites States.

*Corresponding author. Tel.: +82 880 7438.

E-mail address: jyi@snu.ac.kr (J. Yi).

Supporting Figures S1-S11

Supporting Figures

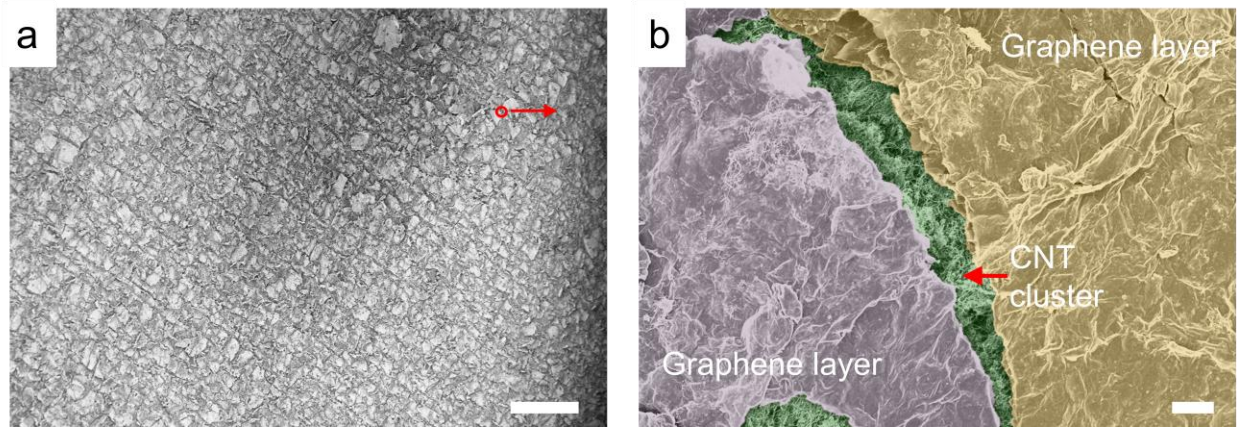

Figure S1. Morphology of the graphene-CNT electrode. (a) SEM image of the surface of graphene-CNT layered electrode. Scale bar is 200 μm. (b) High-resolution SEM image of the graphene-CNT electrode. The graphene layers are separated from each other and are on a CNT cluster. The CNT cluster can withstand bending and stretching.[15] Scale bar is 2 μm.

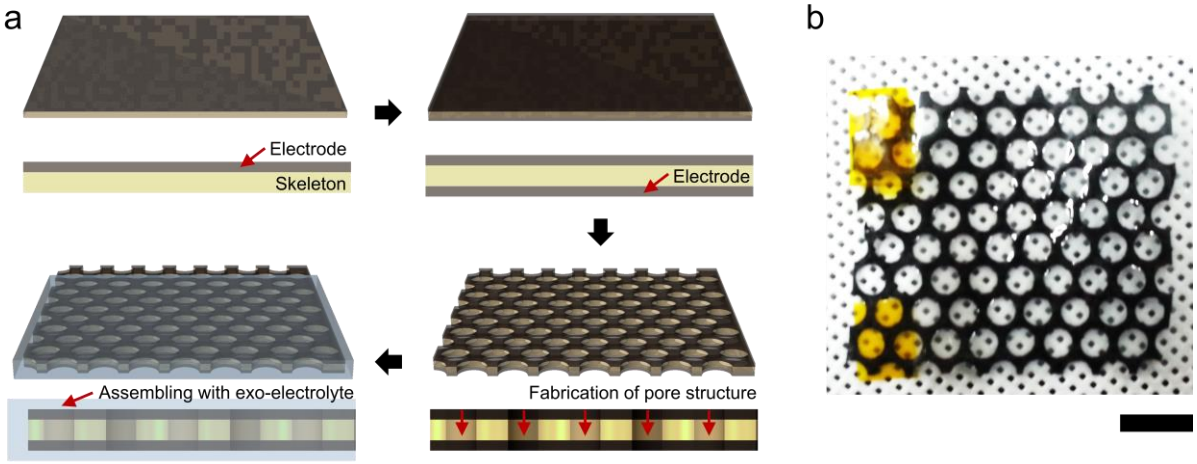

Figure S2. Fabrication of an endoskeleton energy storage system (a) Process flow for fabricating an endoskeleton system (b) Photographs of an endoskeleton energy storage system. Scale bar is 1 cm. Yellow regions are external circuit contact regions on electrodes.

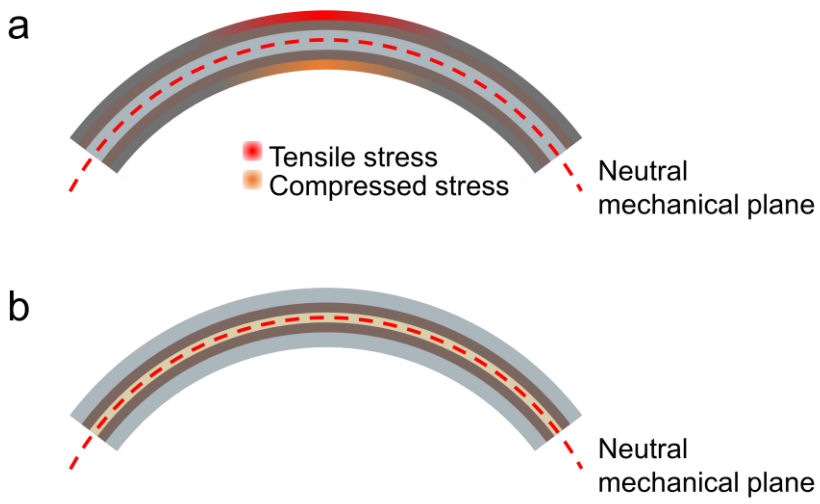

Figure S3. Bending deformation states of energy storages. (a) Exoskeleton system and (b) endoskeleton system.

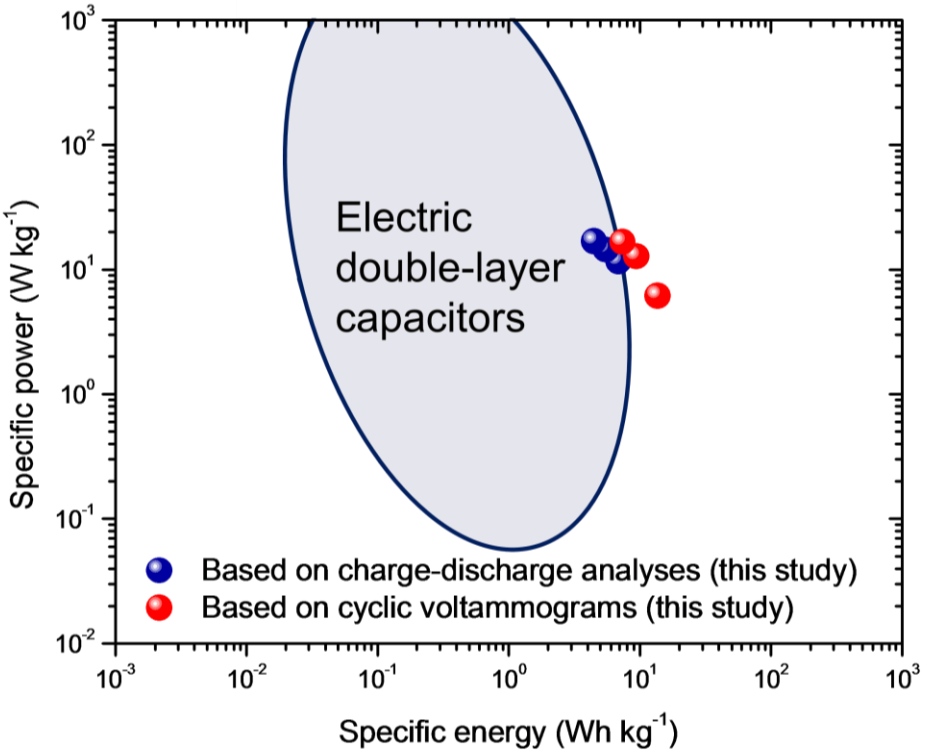

Figure S4. The comparison of specific energy and power of endoskeleton system with conventional electric double layer capacitors.[30-32] Blue dots were derived by charge-discharge analyses and red dots were derived by cyclic voltammograms.

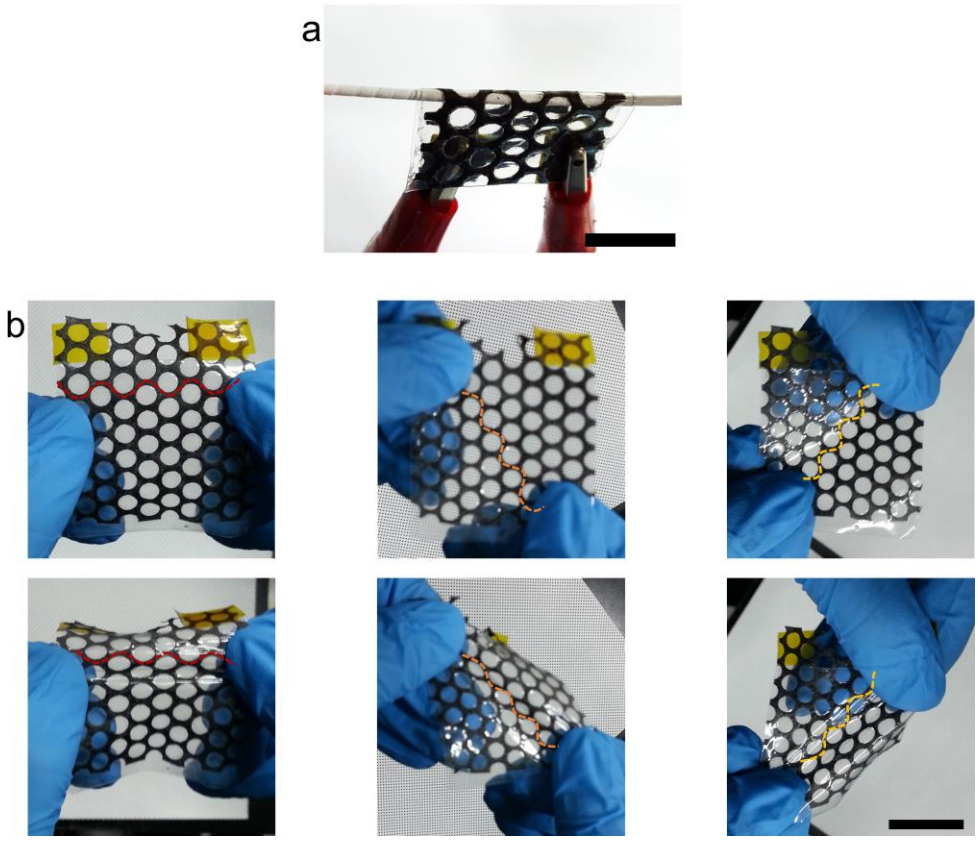

Figure S5. Deformation states of an endoskeleton energy storage system. (a) Bending of an endoskeleton system. The bending radius is 0.5 mm and the scale bar is 10 mm. (b) Stretching of an endoskeleton system at an interval of π/3 radian. There are three serpentine lines with different directions. Scale bar is 20 mm.

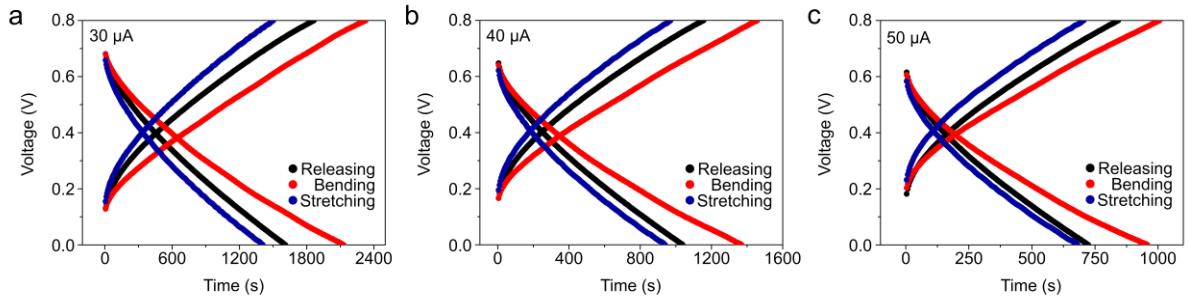

Figure S6. Galvanostatic charge/discharge analyses of an endoskeleton energy storage device at various deformations. The current is (a) 30, (b) 40 and (c) 50 μA. At current of 30 μA, the coulombic efficiencies of the energy storage device are 86, 92 and 94% in releasing, bending and stretching deformation, respectively. At current of 40 μA, the values were 90, 94 and 97% and at 50 μA, the values were 86, 95 and 96% for the different deformations, respectively.

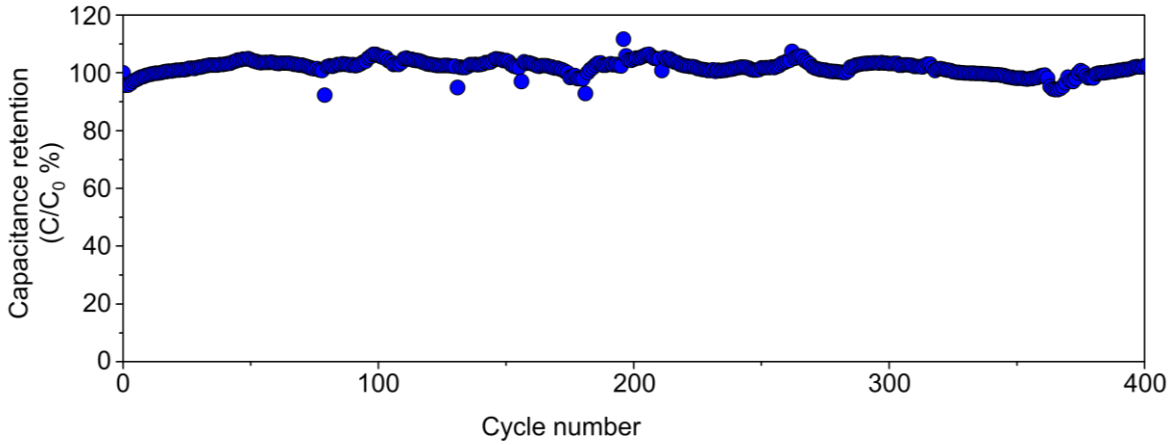

Figure S7. Long cycle stability test of an energy storage device including the endoskeleton during 400 charge-discharge cycles. A retention of ~100% was obtained after 400 cycles.

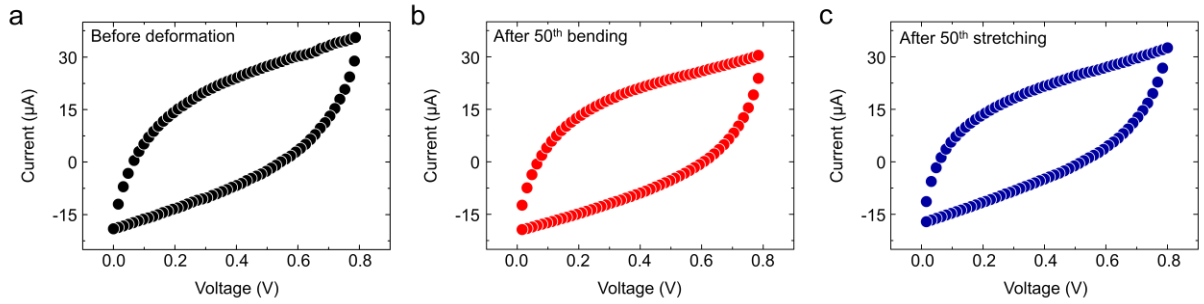

Figure S8. Cyclic voltammograms of the endoskeleton system before and after a series of deformations. (a) before deformation, (b) after 50 bending deformations and (c) after 50 stretching deformations. The scan rate is 1 mV s^{-1}.

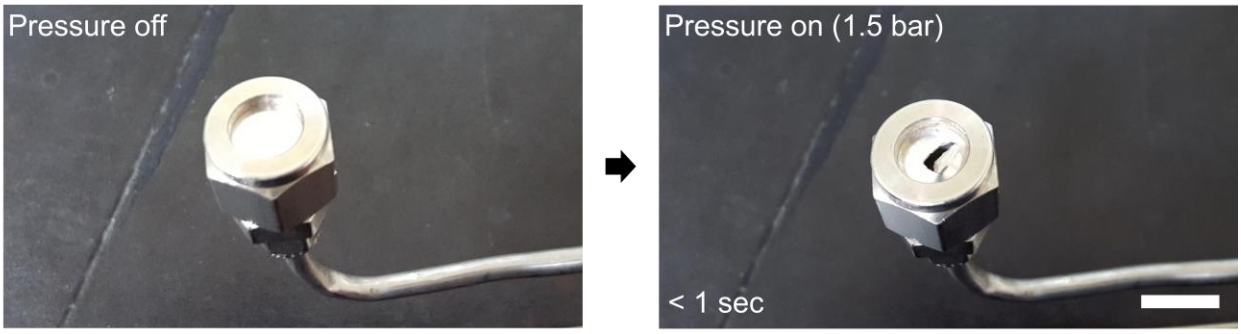

Figure S9. States of a conventional scaffold with CO_2 pressure difference in and out on the surface. The deformation state of a conventional scaffold, Al foil, with and without CO_2 pressure between the inside and outside surface. The relative pressure is 1.5 bar and scale bar is 10 mm.

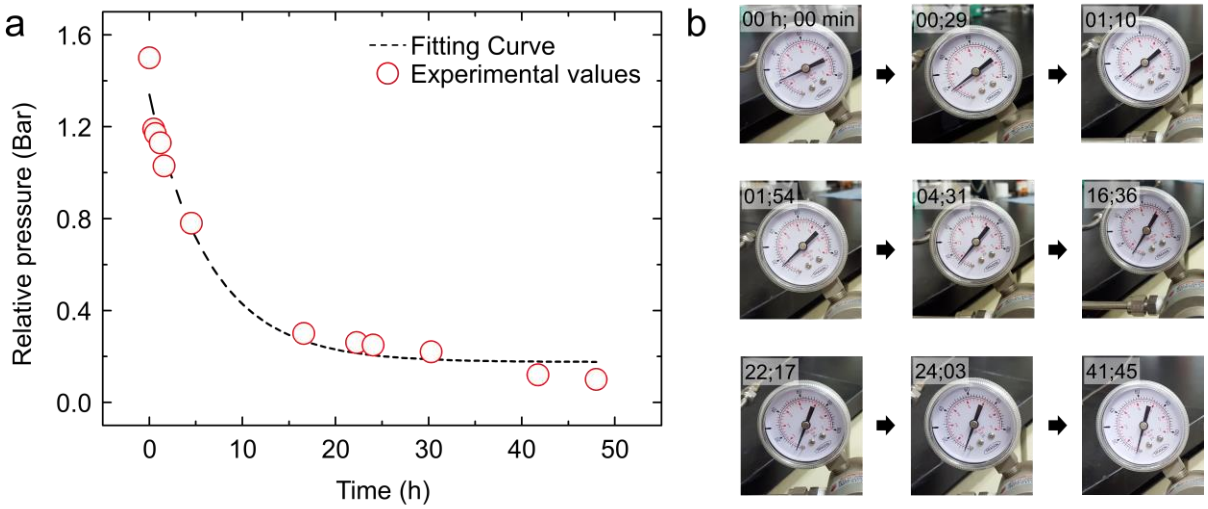

Figure S10. Relative CO_2 pressure between the inside and outside GPE surface as a function of process time. (a) Plot and (b) gauges of relative CO_2 pressure versus process time.

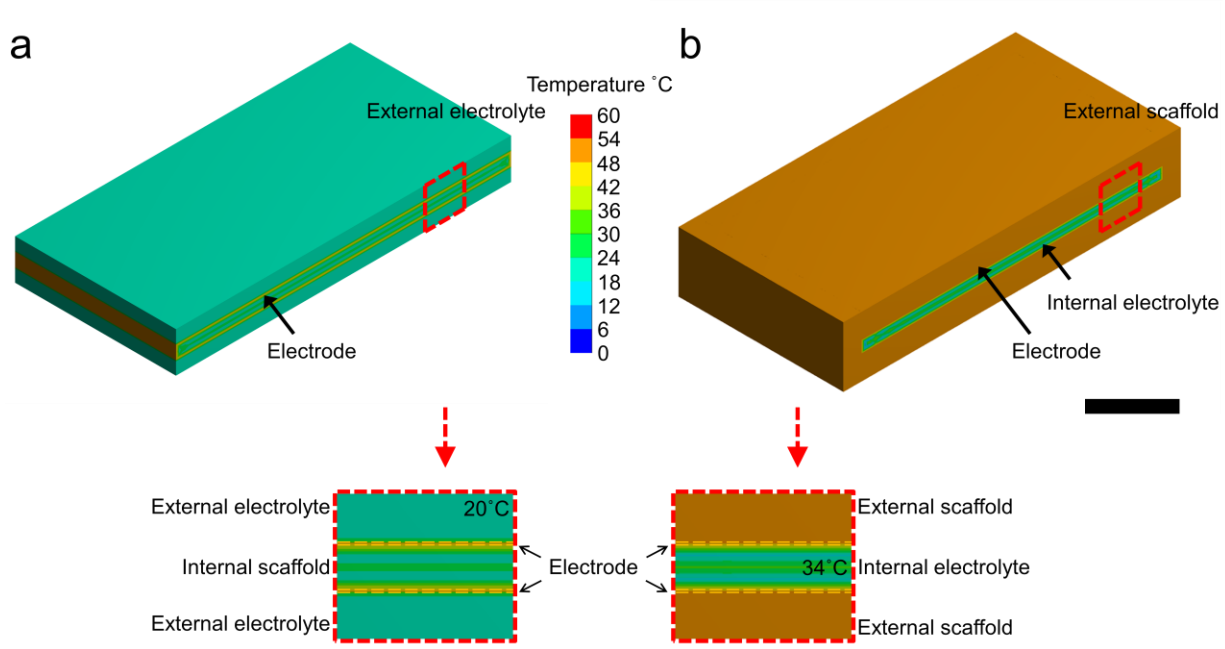

Figure S11. Temperature distributions in endoskeleton *versus* exoskeleton systems. (a) Temperature distribution of an endoskeleton system (b) Temperature distribution of an exoskeleton system. The temperatures were calculated by transient thermal simulation. The initial temperature on the electrode surface was 50 ˚C and transient time was one second. Scale bar is 10 mm.